

The low-temperature interaction of NH₃/NO/NO₂ + O₂ with Fe-ZSM-5 + BaO/Al₂O₃ and H-ZSM-5 + BaO/Al₂O₃: Influence of phase separation and relevance for the NH₃-SCR chemistry

Tommaso Selleri, Isabella Nova, Enrico Tronconi *

Dipartimento di Energia, Laboratorio di Catalisi e Processi Catalitici, Politecnico di Milano, Via La Masa 34, I-20156 Milano, Italy

In an effort to elucidate mechanism and intermediates of Standard SCR over metal-zeolite catalysts, we apply Transient Response Methods (TRM) to identify the mediating species in the low-temperature (120 °C) interaction of NO₂ + O₂, NO + O₂ and NO + NO₂ + O₂ (NO/NO₂ = 10/1 v/v) with a composite Fe-ZSM-5 (Fe = 1% w/w) + BaO/Al₂O₃ system in different configurations (physical mixture versus double-bed), corresponding to different degrees of separation of the two component phases. The results clearly indicate for the first time that the strong interaction between the two system components, already demonstrated in previous work, survives their complete segregation, proceeds via the gas phase, and is mediated by stable gaseous NOx species. The nature of the NOx species trapped on the BaO phase is identified by TPD experiments: in line with previous data, they include primarily nitrates for NO₂ adsorption, and nitrites for NO + O₂ adsorption at short exposure times. A new, striking finding is that formation of nitrites on BaO upon exposure of Fe-ZSM-5 + BaO/Al₂O₃ to NO + O₂, which involves the oxidative activation of NO on Fe-sites, is fully equivalent to the formation of nitrites observed upon exposing only BaO/Al₂O₃ to NO₂ in excess NO. This suggests that NO₂ (possibly in the form of N₂O₃) may play the role of mediating gas-phase species generated by the oxidative activation of NO on Fe centers. The reactivity with NH₃ of nitrites trapped on BaO is probed by Temperature Programmed Surface Reaction (NH₃-TPSR) runs, which show rapid dinitrogen formation from low temperatures when Fe-ZSM-5 is not only mixed with, but also placed downstream from BaO/Al₂O₃, thus confirming the stability of the NOx intermediate formed on Fe-centers, and linking it to the Standard SCR reactivity. Finally, in order to study the role of the metal redox sites in the reactivity of nitrites stored on BaO with ammonia, we compare NH₃-TPSR experiments over a Fe-ZSM-5 catalyst and over a parent H-ZSM-5 zeolite with a drastically reduced Fe content (Fe ≈ 0.02% w/w). Results show that nitrites on BaO react with NH₃ to dinitrogen equally well on Fe- and on H-ZSM-5, which questions the role of the metal sites and therefore of the oxidative activation of NH₃ in such a step.

The present data emphasize the bifunctional (redox + acid) nature of the NH₃-SCR catalytic chemistry at low temperatures, and should be considered in the development of comprehensive mechanisms for the Standard SCR reaction over Fe-zeolite catalysts.

Keywords: NO oxidation, Standard SCR mechanism, Fe-zeolite catalyst, Nitrates, Nitrites, Chemical trapping

1. Introduction

Emissions regulations for both compression and spark-ignited internal combustion engines are becoming more stringent worldwide, as it is no longer possible to achieve the limits imposed by international legislation by just improving the combustion technology. For lean burn Diesel engines, in particular, the NH₃/Urea-Selective Catalytic Reduction process (NH₃/Urea-SCR)

has been successfully demonstrated at the commercial scale and currently represents the best available technology for NOx abatement. In NH₃-SCR converters, excellent deNOx performances are attained over metal-promoted zeolite catalysts thanks to their high activity in two main reactions, namely the Standard SCR reaction (NO + O₂ + NH₃) and the Fast SCR reaction (NO + NO₂ + NH₃) [1].

The elucidation of the SCR catalytic mechanisms over state-of-the-art metal-exchanged zeolites has been a central research topic in recent years [1–16] but, particularly for what concerns the Standard SCR reaction, a comprehensive and satisfactory account is still lacking. In recent publications we have investigated the NO + O₂ adsorption on physical mixtures of metal (Fe and Cu) promoted zeo-

Article history:

Received 1 November 2016

Received in revised form 5 January 2017

Accepted 12 January 2017

Available online 17 January 2017

* Corresponding author.

E-mail address: enrico.tronconi@polimi.it (E. Tronconi).

lites and BaO/Al₂O₃ [12–14], with the aim of providing new insight in the catalytic chemistry of the low-temperature Standard SCR. In these works, we succeeded in trapping onto the BaO/Al₂O₃ phase unstable nitrites generated by the oxidative activation of NO on the metal-zeolite catalyst, and we speculated on the possible existence of a gas-phase pathway responsible for the observed interaction between the two physical mixture components. Nitrites storage on BaO was demonstrated in several ways, including: (i) their thermal decomposition to an equimolar mixture of NO and NO₂ during TPD, (ii) N₂ formation during their reaction with NH₃ at low temperature, (iii) ex-situ IR analysis of the BaO/Al₂O₃ phase after unloading and separation from the mechanical mixture.

In the present work, we further investigate the interaction of NO_x + O₂ with composite Fe-ZSM-5 + BaO/Al₂O₃ systems on the basis of a completely new set of data, with the dual goal of clarifying whether such an interaction proceeds indeed via gas phase, and of identifying the involved mediating species. To this purpose, herein we analyze the effect of phase segregation on the synergy between the two component phases. In particular, we have focused on the following configurations: (i) mechanical mixture with the two phases in loose contact; (ii) sequential segregated beds, where the two components (positioned in different orders) are separated by an inert quartz wool layer; (iii) single constituents of the mixture, individually tested.

The pathway leading to the trapping of nitrites on BaO is clearly relevant for the NO activation step in the Standard SCR chemistry, as discussed in the following paragraphs. To complete the analysis of the Standard SCR mechanism, herein we also investigate the subsequent reactivity of nitrites with NH₃, and perform dedicated experiments on H-ZSM-5 to clarify the role of redox Fe centers in this second stage of the mechanism.

Altogether, the present experimental results are significant for the elucidation of the Standard SCR reaction chemistry over Fe-promoted zeolites, provide new elements for the development of a comprehensive SCR mechanism, and may be useful to discriminate rival mechanistic proposals.

2. Experimental

In this study, different systems comprising a Fe-ZSM-5 zeolite (22 mg), an H-ZSM-5 zeolite (22 mg) and in-house prepared BaO/Al₂O₃ (44 mg), all in form of powders, were tested in different spatial arrangements. The Fe-ZSM-5 was a commercial catalyst manufactured by Zeolyst (CP 7117), with a SiO₂/Al₂O₃ ratio of 24, surface area of 300 m²/g and 1% w/w Fe content. The H-ZSM-5 sample was a commercial material manufactured by Zeolyst (CBV 2314), with a SiO₂/Al₂O₃ ratio of 23, surface area of 425 m²/g and 0.05% w/w Na₂O content. ICP-MS analysis revealed a residual Fe content of 0.0235% w/w, i.e. significantly lower (over 40 times) with respect to the Fe-exchanged catalyst. Both zeolite powders were dried at 120 °C for 1 h and sieved to 120–140 mesh (average particle size = 115 µm). The BaO/Al₂O₃ component (Ba content = 16% w/w) was prepared in-house by incipient wetness impregnation, using aqueous solutions of Ba(CH₃COO)₂ (Sigma Aldrich, 99% pure) to impregnate the γ-alumina support (Versal 250 from Eurosupport: surface area = 200 m²/g and pore volume = 1.2 cm³/g) calcined at 800 °C. After impregnation, the powder was dried at 80 °C overnight, calcined at 500 °C for 5 h, and sieved to 140–200 mesh (average particle size = 90 µm). Cordierite with 120–140 mesh size was added for dilution. In all runs, the powders were loaded in a quartz microflow reactor (ID = 7 mm). The following configurations have been tested: (i) a physical mixture of Fe-ZSM-5 and BaO/Al₂O₃ powders (identified in the following as Fe-Ba-MM) with the two phases in loose contact and a total dilution with cordierite up to 120 mg; (ii) a double-bed configuration with Fe-ZSM-5 first,

followed by a BaO/Al₂O₃ layer (identified in the following as Fe-Ba-DB); (iii) reverse double-bed configurations with BaO/Al₂O₃ first, followed by a layer of either Fe-ZSM-5 or H-ZSM-5 (identified in the following as Ba-Fe-DB or Ba-Z-DB, respectively). In the double-bed configurations, the two phases were completely separated by a quartz wool plug, and each layer was diluted with cordierite up to 60 mg. For completeness, the three components (Fe-ZSM-5, BaO/Al₂O₃ and H-ZSM-5) were also tested individually after dilution up to a total bed load of 120 mg.

Before running any test, each new sample was conditioned once for 5 h at 600 °C in a continuous flow of 10% v/v H₂O and 10% v/v O₂ in He. Moreover, prior to every experiment the powders were pre-treated feeding 8% v/v O₂ + He at 550 °C continuously for 1 h and then also during the cool-down transient to the test temperature (120 °C). For brevity, illustration of the pre-treatment process is omitted in the results shown here: the data acquisition started (*t* = 0) when the desired test temperature was reached. The feed mixture to the reactor was composed from calibrated NO + He, NO₂ + He, NH₃ + He, O₂ + He mixtures in gas bottles using several mass flow controllers (Brooks Instruments). In particular, NO and O₂ were fed to the reactor via independent lines and mixed just before the reactor inlet, in order to prevent formation of NO₂ upstream of the catalyst bed. The purity of the mixtures was checked by a UV analyzer during preliminary calibrations. The gas species concentrations at the reactor outlet were analyzed by a quadrupole mass spectrometer (Balzers QMS 200) and a UV analyzer (ABB LIMAS 11 HW) arranged in a parallel configuration or, in an upgraded alternative set-up, using a new quadrupole mass spectrometer (Hiden Analytical QGA), which granted significant reduction of the signal noise. Cross-check experiments gave however essentially identical results in the two rigs.

The experimental protocol herein adopted is similar to the one described and validated in our previous works [12–14]. In general, three different types of transient gas-phase experiments were performed: (i) isothermal adsorption of a mixture of NO + O₂, or NO₂ + O₂ or NO + NO₂ + O₂, followed by Temperature Programmed Desorption (TPD) in He; (ii) isothermal adsorption of the same gas mixtures followed by Temperature Programmed Surface Reaction (TPSR) with NH₃; (iii) isothermal adsorption of NH₃ followed by Temperature Programmed Surface Reaction (TPSR) with NO + NO₂. Unless otherwise indicated, all the tests were run with an overall volumetric flow rate of 120 cm³/min (STP) at an adsorption temperature of 120 °C under dry conditions. Our previous works, in fact, pointed out a strong negative impact of H₂O on the amount of NO_x trapped on BaO due to its inhibitory action both on the NO oxidation activity of Fe-ZSM-5 [4], as also well known in the literature, and on the nitrites storage on BaO, documented e.g. by a dedicated experiment in [13]. Additional details regarding the experimental set-up and procedures, as well as the preparation and the characterization of the tested samples, can be found in [12–14].

3. Results and discussion

3.1. NO₂ + O₂ adsorption/TPD tests

In the isothermal adsorption phases, not shown here for brevity, 500 ppm of NO₂, 8% O₂ and balance He were fed to the reactor until saturation at 120 °C. Fig. 1A shows the thermal decomposition (TPD) profiles of the NO_x species stored on the investigated composite systems, namely Fe-Ba-MM, Fe-Ba-DB, and Ba-Fe-DB. For comparison, the results obtained in previous work [13] on the individually tested component phases are also displayed in Fig. 1B.

For all the three combined systems, Fig. 1A shows that the adsorbed NO_x species decompose mainly to NO₂, as expected in the case of nitrates storage [13,14]. The formation of stable nitrates

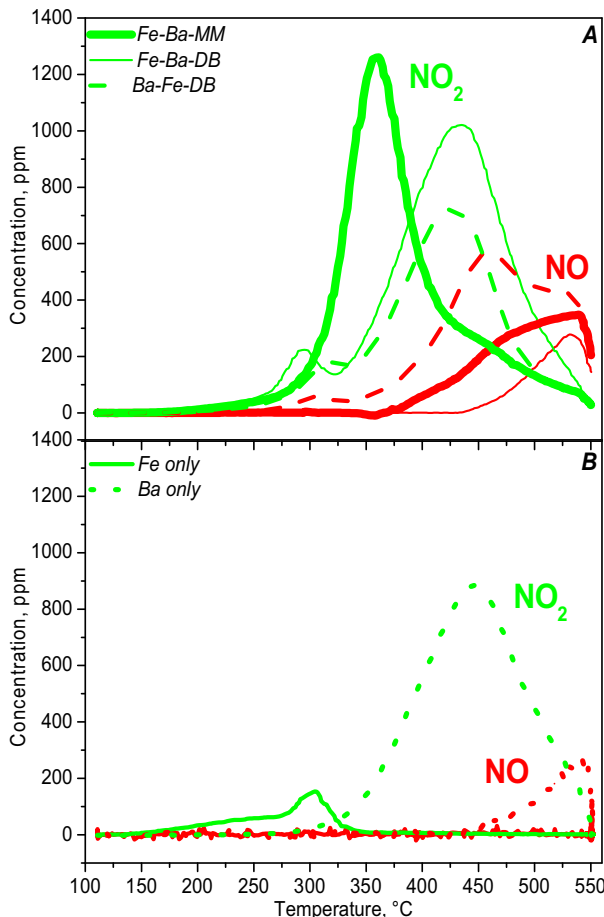


Fig. 1. TPD runs in He ($T = 120\text{--}550\text{ }^{\circ}\text{C}$; heating rate = $15\text{ }^{\circ}\text{C}/\text{min}$) following $\text{NO}_2 + \text{O}_2$ adsorption at $120\text{ }^{\circ}\text{C}$ ($\text{NO}_2 = 500\text{ ppm}$; $\text{O}_2 = 8\%$) on: (A) Fe-ZSM-5 + $\text{BaO}/\text{Al}_2\text{O}_3$ in different configurations (thick lines: Fe-Ba-MM; thin lines: Fe-Ba-DB; dashed lines: Ba-Fe-DB); (B) individually tested Fe-ZSM-5 (solid lines) and $\text{BaO}/\text{Al}_2\text{O}_3$ (dotted lines), reported for reference [13,14].

upon exposure of the same Fe-ZSM-5 catalyst to NO_2 was in fact demonstrated by *in situ* FTIR in a previous dedicated study [16]. At temperatures above $400\text{ }^{\circ}\text{C}$, NO evolution is also detected, in line with the occurrence of NO_2 decomposition to $\text{NO} + \text{O}_2$ [13,14,17]. As already reported for mechanical mixture configurations [13,14], the NO_2 TPD trace associated with Fe-Ba-MM (Fig. 1A, thick lines) exhibits a big peak (1260 ppm) centered at about $360\text{ }^{\circ}\text{C}$. Interestingly, this peak temperature is approximately $90\text{ }^{\circ}\text{C}$ lower than the one registered in the same NO_2 adsorption experiment on $\text{BaO}/\text{Al}_2\text{O}_3$ alone ($450\text{ }^{\circ}\text{C}$), see Fig. 1B. Thus, the thermal stability of barium nitrates is less in the mechanical mixture configuration, likely due to the presence of the iron sites. In fact, as also evident in Fig. 1B, Fe nitrates start to decompose at lower temperatures (around $200\text{ }^{\circ}\text{C}$), freeing active sites that may act as additional decomposition centers for nitrates stored on $\text{BaO}/\text{Al}_2\text{O}_3$. This is clear evidence for an interaction between the two mixture components, and strongly suggests that Ba- and Fe-nitrates are both in equilibrium with a mediating gas-phase species, possibly HNO_3 or NO_2 .

Upon separating the mixture components in two segregated beds, with Fe-ZSM-5 upstream of $\text{BaO}/\text{Al}_2\text{O}_3$ (Fe-Ba-DB), the NO_2 TPD trace was changed to a bimodal profile with a first peak of 220 ppm at $300\text{ }^{\circ}\text{C}$ and a second one of 1020 ppm at $435\text{ }^{\circ}\text{C}$ (Fig. 1A, thin lines). In this double bed configuration, therefore, the two components behave independently, with two separate nitrates decomposition peaks corresponding nicely to those observed on

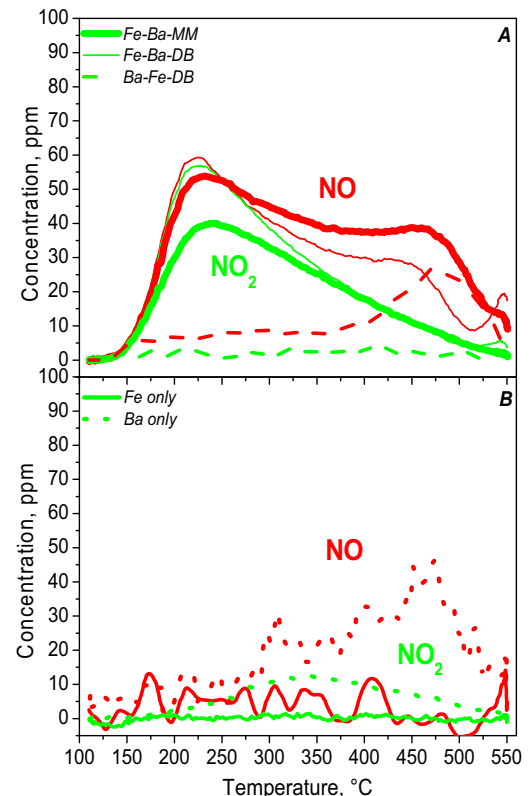


Fig. 2. TPD runs in He ($T = 120\text{--}550\text{ }^{\circ}\text{C}$; heating rate = $15\text{ }^{\circ}\text{C}/\text{min}$) following $\text{NO} + \text{O}_2$ adsorption at $120\text{ }^{\circ}\text{C}$ ($\text{NO} = 500\text{ ppm}$; $\text{O}_2 = 8\%$) on: (A) Fe-ZSM-5 + $\text{BaO}/\text{Al}_2\text{O}_3$ in different configurations (thick lines: Fe-Ba-MM; thin lines: Fe-Ba-DB; dashed lines: Ba-Fe-DB); (B) individually tested Fe-ZSM-5 (solid lines) and $\text{BaO}/\text{Al}_2\text{O}_3$ (dotted lines), reported for reference [12,13].

the individually tested systems, shown in Fig. 1B. In this case, no interaction is evident: on the contrary, the NO_2 TPD profile is just the superposition of those obtained on the two single components, which is indeed consistent with the arrangement of the two layers in the Fe-Ba-DB system. In fact, the Fe-ZSM-5 bed is positioned upstream, so, unlike in the mechanical mixture, the redox metal sites cannot act as decomposition centers for the stable Ba nitrates, which are stored in the downstream layer. Indeed, the synergistic effect is absent also when reversing the order of the layers (Ba-Fe-DB), as clearly seen in Fig. 1A (dashed lines). Again, phase separation prevents the shift of the local nitrates decomposition equilibrium, differently from the case of the mechanical mixture (Fe-Ba-MM). The different NO_2 release concentrations noted e.g. between $\text{BaO}/\text{Al}_2\text{O}_3$ and Ba-Fe-DB are likely explained by the differences in the overall NO_x storage capacity of $\text{BaO}/\text{Al}_2\text{O}_3$ samples from replicated preparations.

In summary, the NO_2 adsorption/TPD tests point out a significant interaction between the two component phases of our composite systems during nitrates decomposition, but only in the case of Fe-Ba-MM. In fact, the nitrates stored onto BaO are more easily decomposed only when BaO is mixed with Fe-ZSM-5. Such an interaction apparently requires proximity of the Fe decomposition sites to the BaO storage sites.

3.2. $\text{NO} + \text{O}_2$ adsorption/TPD tests

In the isothermal adsorption phases of these experiments, not shown here for brevity, 500 ppm of NO with 8% O_2 and balance He were fed to the reactor until saturation at $120\text{ }^{\circ}\text{C}$. Fig. 2A shows the TPD profiles of the NO_x species stored on the investigated composite systems, i.e. Fe-Ba-MM, Fe-Ba-DB, and Ba-Fe-DB, after exposure

to $\text{NO} + \text{O}_2$. For comparison, the corresponding results obtained in previous work [12–14] on the individually tested components are also displayed in Fig. 2B. Contrary to the case of NO_2 adsorption, the stored NOx species exhibit here the typical thermal decomposition behavior of nitrites, i.e. equimolar release of NO and NO_2 in the low temperature region [12–14], with the exception of the Ba-Fe-DB configuration, explained later.

As also discussed extensively in [12–15], a clear synergistic interaction between Fe-ZSM-5 and $\text{BaO}/\text{Al}_2\text{O}_3$ is again evident when comparing the mechanical mixture (Fe-Ba-MM) in Fig. 2A (thick lines) to the individual components, reported for reference in Fig. 2B. The NO and NO_2 TPD traces are overlapped until 180 °C, with a main peak at 225 °C. These results are explained considering that NO is oxidatively activated on Fe sites and the generated intermediates are trapped on the $\text{BaO}/\text{Al}_2\text{O}_3$ phase in the form of barium nitrites. Indeed, Fig. 2B clearly confirms that the NOx storage on the two individual components is quite small: in fact, Fe-ZSM-5 is not able to stabilize nitrites which easily decompose, while $\text{BaO}/\text{Al}_2\text{O}_3$ has a very limited oxidation activity and is thus unable to activate NO.

When $\text{NO} + \text{O}_2$ adsorption was replicated on the Fe-ZSM-5 + $\text{BaO}/\text{Al}_2\text{O}_3$ double bed configuration (Fe-Ba-DB, see Fig. 2A, thin lines), almost identical decomposition profiles were obtained as over the mechanical mixture (Fe-Ba-MM): NO and NO_2 were released in perfect equimolar proportions up to 300 °C, with a peak of about 60 ppm each at 225 °C. Thus, remarkably, the synergy between the Fe-ZSM-5 catalyst and $\text{BaO}/\text{Al}_2\text{O}_3$ during $\text{NO} + \text{O}_2$ adsorption is completely unaffected by the segregation of the two phases. This implies that the interaction proceeds via the gas phase and is mediated by a stable molecule, which is obviously a nitrite precursor and therefore different from the NO_2 adsorption case. These results are apparently at variance with those obtained by Salazar et al. [18] on hybrid catalysts containing an oxidation component (e.g. Mn_2O_3 , hopcalite and Ce-ZrO_x) and an SCR component (Fe-ZSM-5, V_2O_5 - WO_3 / TiO_2) arranged in either physical mixtures or segregated configurations. In their work, the authors observed a strong increase of the Standard SCR performances on the combined system with close contact between the two phases, possibly due to the beneficial effect of the oxidation component in the oxidative activation of NO. However, the synergy was strongly reduced in a loose contact physical mixture and completely absent in more segregated configurations, suggesting that the interaction, in this case, was mediated by a labile intermediate [18].

Finally, upon reversing the order of the layers (Ba-Fe-DB) in Fig. 2A (dashed lines), no significant storage of nitrites was noted, as expected also from previous results [13]. In this case, the TPD curves look very similar to those shown in Fig. 2B for the individual systems. In fact, here Fe-ZSM-5 is placed downstream of the storage material, which prevents trapping of any nitrites precursors formed over the oxidative component.

Thus, oxidative activation of NO at 120 °C over Fe-ZSM-5 generates a stable gas-phase nitrite precursor, which can travel a significant distance across the reactor to reach the segregated BaO component downstream, and is eventually trapped as a stable Ba nitrite. At this point, of course, the question is about the nature of such a mediating gaseous species, which could possibly be NO_2 , N_2O_3 or HONO [7,8,12–14]. The answer is quite relevant for the elucidation of the Standard SCR mechanism.

3.3. $\text{NO} + \text{NO}_2 + \text{O}_2$ adsorption/TPD tests

The following experiment was performed to gain insight in the nature of the gas-phase species mediating the synergy of combined Fe-ZSM-5 + $\text{BaO}/\text{Al}_2\text{O}_3$ systems in $\text{NO} + \text{O}_2$ adsorption. The Fe-zeolite catalyst, whose role is to oxidatively activate NO, was removed from the tested system and its functionality was replaced

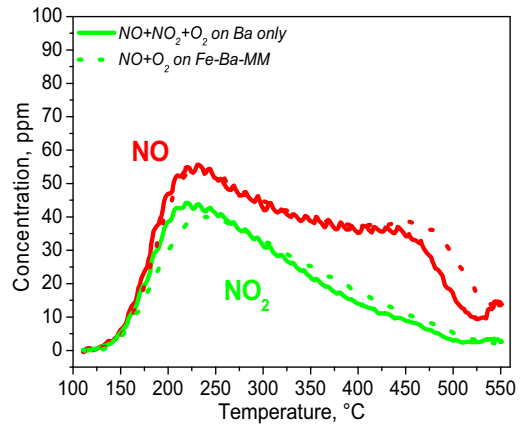


Fig. 3. TPD runs in He ($T=120\text{--}550^\circ\text{C}$; heating rate = 15 °C/min) following $\text{NO} + \text{NO}_2 + \text{O}_2$ adsorption at 120 °C (NO = 500 ppm; NO_2 = 50 ppm; O_2 = 8%, exposure time = 45 min) on $\text{BaO}/\text{Al}_2\text{O}_3$ only (solid lines) and $\text{NO} + \text{O}_2$ adsorption at 120 °C (NO = 500 ppm; O_2 = 8%) on Fe-ZSM-5 + $\text{BaO}/\text{Al}_2\text{O}_3$ physical mixture (Fe-Ba-MM, dotted lines), respectively.

by adding 50 ppm of NO_2 to the 500 ppm $\text{NO} + 8\%$ O_2 mixture fed to $\text{BaO}/\text{Al}_2\text{O}_3$ only. This was the minimum concentration of NO_2 that could be fed to the reactor due to experimental constraints: it is, however, in the same order of magnitude of the steady-state outlet NO_2 concentration generated by the NO oxidation activity of the Fe-BaO physical mixture [12,13]. The TPD curves following $\text{NO} + \text{NO}_2 + \text{O}_2$ adsorption on $\text{BaO}/\text{Al}_2\text{O}_3$ are plotted in Fig. 3 as solid lines. NO and NO_2 were desorbed in equimolar amounts up to 180 °C, with synchronous peaks at 225 °C, again in line with nitrites thermal decomposition. This confirms that exposure to a mixture of NO_2 in excess NO can form nitrites on $\text{BaO}/\text{Al}_2\text{O}_3$, as already pointed out by Iglesia et al. [19]. It is also worth noticing here that the duration of $\text{NO} + \text{O}_2$ adsorption on $\text{BaO}/\text{Al}_2\text{O}_3$ was controlled and limited to 45 min to prevent the consecutive oxidation of the trapped nitrites to nitrates by NO_2 [19], see Section 3.5 below. Notably, we can also rule out the initial formation of nitrates on $\text{BaO}/\text{Al}_2\text{O}_3$ and their subsequent reduction by NO to nitrites based on a dedicated test, already presented in [13]. In this test, a single bed of $\text{BaO}/\text{Al}_2\text{O}_3$ was first saturated with nitrates at 120 °C, and subsequently exposed to 500 ppm of NO without observing any appreciable reaction.

As a most interesting and surprising result, however, Fig. 3 further shows that the TPD curves recorded after $\text{NO} + \text{NO}_2 + \text{O}_2$ isothermal adsorption on $\text{BaO}/\text{Al}_2\text{O}_3$ (solid lines) almost perfectly match the TPD curves obtained following $\text{NO} + \text{O}_2$ adsorption on the Fe-Ba-MM physical mixture, also displayed as dotted lines for comparison. Thus, adsorption of NO_2 in excess NO on the BaO phase alone results in a storage of nitrites that is both qualitatively and quantitatively similar to what observed in $\text{NO} + \text{O}_2$ adsorption runs on both mechanical mixture (Fe-Ba-MM) and double-bed (Fe-Ba-DB) systems. The simplest possible explanation of this new compelling result is that the role of Fe sites in Fe-ZSM-5 is to oxidize NO to NO_2 . According to this interpretation, NO_2 would be therefore the stable mediating gaseous species involved in the interaction between Fe-ZSM-5 and $\text{BaO}/\text{Al}_2\text{O}_3$ pointed out in the previous paragraphs.

Another experiment apparently corroborating this interpretation is presented in Fig. 4. It involves an isothermal step feed of 2% O_2 during continuous feed of NO at 120 °C on Fe-ZSM-5 only (dashed lines) and on the Fe-ZSM-5 + $\text{BaO}/\text{Al}_2\text{O}_3$ double bed system (Fe-Ba-DB, solid lines). Fig. 4 shows that as soon as oxygen was fed to Fe-ZSM-5, approximately 50 ppm of NO were converted and

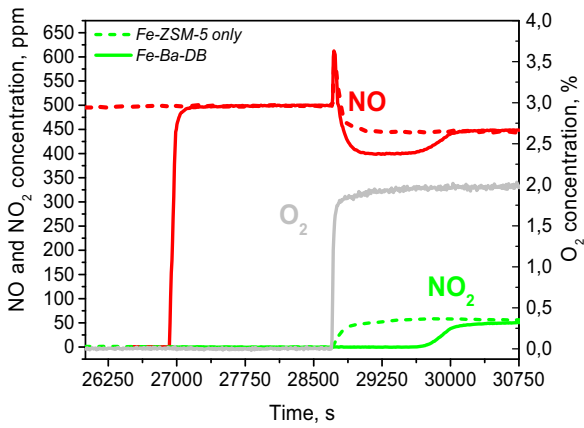


Fig. 4. O₂ step feed during NO isothermal adsorption (T=120 °C; NO=500 ppm; O₂=2%) on Fe-ZSM-5+BaO/Al₂O₃ double bed (solid lines) and on Fe-ZSM-5 only (dashed lines).

50 ppm of NO₂ were produced, in line with the occurrence of NO oxidation, (R1) [12,13]:



When the same experiment was run on Fe-Ba-DB, different, peculiar dynamics were observed: the NO outlet concentration first dropped to 400 ppm and then, after a transient, recovered the same steady state value noticed in the case of Fe-ZSM-5 only (\approx 450 ppm). This is quantitatively in line with one molecule of NO being oxidized to NO₂ on the Fe-zeolite, (R1), which is then trapped, together with one additional NO molecule, as barium nitrite in the BaO-Al₂O₃ bed downstream according to (R2), until saturation equilibrium is reached:



Integral analysis confirmed storage of similar amounts of NOx after the NO+O₂ adsorption on Fe-Ba-DB (Fig. 4), the NO+O₂ adsorption on Fe-Ba-MM (Fig. 2), and the NO+NO₂+O₂ adsorption on BaO/Al₂O₃ (Fig. 3).

3.4. Discussion on the nature of the intermediate species in NO+O₂ adsorption

Even though the new results presented in the previous paragraphs apparently suggest that NO₂ acts as the mediating species between Fe-ZSM-5 and BaO, we believe that the identification of the intermediate formed by the oxidative activation of NO over Fe-zeolites is not so straightforward and deserves some more detailed discussion. Indeed, the simple scheme with NO oxidation to NO₂ as the rate determining step of Standard SCR has been questioned in the past by some of us on the basis of multiple kinetic pieces of evidence [4].

Our present data tell clearly that the intermediate generated by NO oxidation on Fe-centers has to be a nitrite precursor, since its interaction with BaO results in the formation of nitrites as primary adsorbed species [13,14]. In the NO₂ molecule, however, N has a formal oxidation state of 4+, while in nitrites N has a formal oxidation state of 3+, so pure NO₂ cannot be a direct precursor of nitrites. In the adsorption of NO₂ alone, in fact, NO₂ disproportionates to form both nitrites and nitrates, as discussed e.g. in [16]. However, the results of our NO₂+NO adsorption runs on BaO/Al₂O₃ show that NO₂ in the presence of excess NO behaves indeed as a nitrite precursor. A possible explanation is that NO₂ in excess NO is in equilibrium with N₂O₃, whose N atoms share a formal oxidation state of 3+, like in nitrites. Furthermore, in presence of H₂O, which

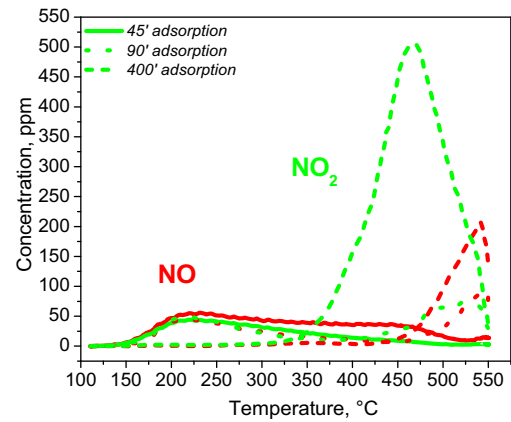


Fig. 5. TPD runs in He (T=120–550 °C; heating rate=15 °C/min) following NO+NO₂+O₂ adsorption (NO=500 ppm; NO₂=50 ppm; O₂=8%) at 120 °C on BaO/Al₂O₃ with different exposure times (thick lines: 45 min; dotted lines: 90 min; dashed lines: 400 min).

cannot be excluded in zeolites even in dry experiments like ours, NO₂+NO may be in equilibrium both with N₂O₃ and with HONO, also a nitrite precursor.

If such equilibria apply, then it seems hardly possible to establish if: (i) NO is first activated on Fe to form ferric nitrites in equilibrium with gaseous N₂O₃/HONO, and subsequently N₂O₃/HONO is stored on BaO as nitrites, or (ii) NO is first oxidized to NO₂ on Fe sites, and then NO+NO₂ are stored on BaO as nitrites. In the future, a kinetic analysis could be attempted to discriminate the two pathways, considering that they might also proceed in parallel.

3.5. Evolution of Ba-nitrites

Fig. 5 compares three TPD profiles following NO+NO₂+O₂ adsorption on BaO/Al₂O₃ with different exposure times. It is evident that, on progressively increasing the adsorption time (from 45 to 400 min), the low-temperature equimolar NO and NO₂ peak, associated with nitrites decomposition, decreased, while two new NO₂ and NO peaks appeared in the high-T region (centered at 525 °C and 550 °C, respectively), associated with the thermal decomposition of stable nitrates to NO₂, which further decomposes to NO+O₂. Accordingly, Fig. 5 highlights the shift towards nitrates with growing NO+NO₂ adsorption time on BaO/Al₂O₃ likely due to the consecutive oxidation of the initially formed nitrites by NO₂, in line with literature indications from Iglesia et al. [19].

3.6. NH₃ reactivity tests

At this point, we look at the subsequent step in the low-temperature Standard SCR chemistry: after NO oxidative activation, the NOx intermediate proceeds to react with NH₃ to form dinitrogen.

We probed the reactivity with NH₃ of nitrites accumulated onto BaO/Al₂O₃ in NO+NO₂+O₂ adsorption tests in NH₃-TPSR experiments on two distinct inverted double bed arrangements, namely Ba-Fe-DB and Ba-Z-DB. In the isothermal adsorption phase of these runs, 500 ppm of NO, 50 ppm of NO₂ and 8% O₂ were fed at 120 °C for a controlled time (45 min) to prevent consecutive oxidation of nitrites to nitrates by NO₂ [19], see also the discussion of Fig. 5. In the second phase, 300 ppm of NH₃ were fed to the reactor at 120 °C until steady state was reached, then the temperature was raised up to 550 °C at 15 °C/min. Fig. 6A shows the subsequent TPSR for the BaO/Al₂O₃+Fe-ZSM-5 double bed configuration (Ba-Fe-DB). As soon as the temperature was increased, N₂ evolution was detected with a peak of approximately 90 ppm at 235 °C. At

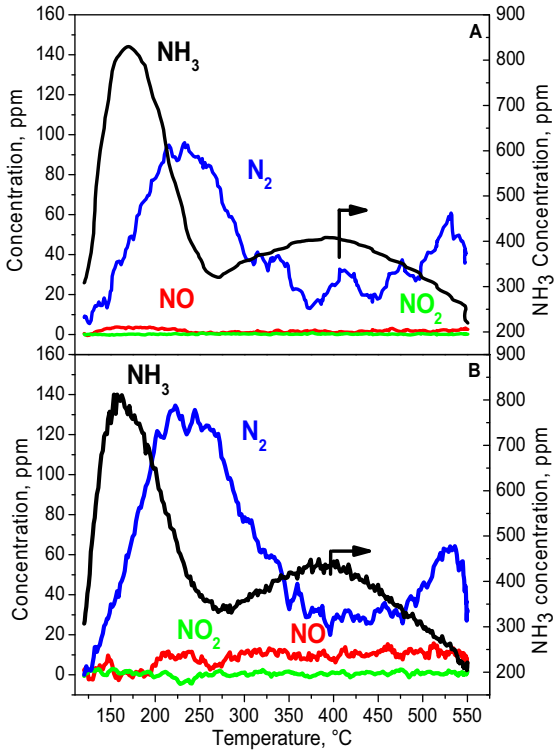


Fig. 6. TPSR runs in NH_3 ($\text{NH}_3 = 300 \text{ ppm}$; $T = 120\text{--}550^\circ\text{C}$; heating rate = $15^\circ\text{C}/\text{min}$) following $\text{NO} + \text{NO}_2 + \text{O}_2$ adsorption at 120°C ($\text{NO} = 500 \text{ ppm}$; $\text{NO}_2 = 50 \text{ ppm}$; $\text{O}_2 = 8\%$) on: (A) Ba-Fe-DB; (B) Ba-Z-DB.

the same time, NH_3 consumption was also observed. The integral amount of produced N_2 ($7.28 \mu\text{mol}$) is consistent with the overall stored $\text{NO} + \text{NO}_2$, evaluated in a dedicated TPD run ($7.84 \mu\text{mol}$), with a balance error below 8%, in line with the well-known Fast SCR stoichiometry, (R3):

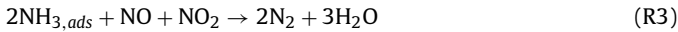


Fig. 6B shows further that a very similar result was found when replacing Fe-ZSM-5 with H-ZSM-5 in the double bed arrangement (Ba-Z-DB). Again, a low temperature N_2 peak of 125 ppm at 235°C , even more abundant than in the previous case, was detected. Also in this case, a limited additional N_2 production peak was noticed at high temperature: this may be explained by the reaction of NH_3 with some nitrates generated by the NO_2 conversion of nitrites, as shown e.g. in **Fig. 5**. Notice that, in both cases, no N_2 was detected when NH_3 was fed to the reactor before starting the ramp, being the temperature (120°C) too low to initiate nitrites decomposition from the $\text{BaO}/\text{Al}_2\text{O}_3$ phase.

The low temperature reactivity with NH_3 noted in the previous tests is typical of nitrites, as well known and already discussed in previous chemical trapping work [12–15] on physical mixtures: we show here that it is still present in a configuration with segregated beds. Notice that only limited NH_3 storage and, most importantly, insignificant NH_3 reactivity were observed on the $\text{BaO}/\text{Al}_2\text{O}_3$ phase when tested alone in the dedicated test presented in **Fig. 7** below.

The NH_3 -TPSR data in **Fig. 6** are strong evidence that the equimolar mixture of NO and NO_2 from decomposition of barium nitrites stored on $\text{BaO}/\text{Al}_2\text{O}_3$ readily reacts with the ammonia adsorbed on the zeolite acid sites downstream. In fact, the behaviors of the two tested samples, namely Ba-Fe-DB and Ba-Z-DB, are essentially identical, even though the Fe contents of the two zeolites differ by two orders of magnitude. Moreover, the reactivity is quite significant, leading to a complete conversion of the stored species, despite the very low temperature. Clearly, such a very effective reactivity is to

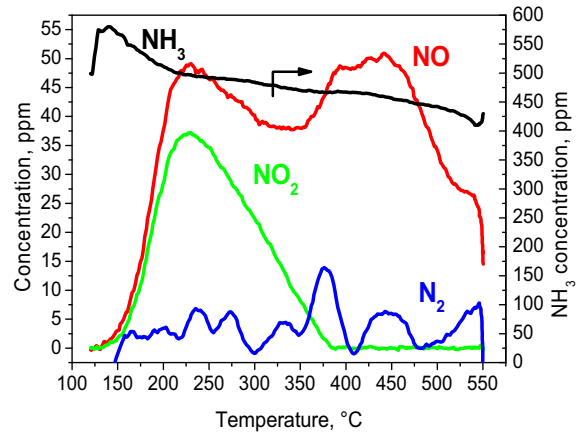


Fig. 7. TPSR run in NH_3 ($\text{NH}_3 = 500 \text{ ppm}$; $T = 120\text{--}550^\circ\text{C}$; heating rate = $15^\circ\text{C}/\text{min}$) following $\text{NO} + \text{NO}_2 + \text{O}_2$ adsorption ($\text{NO} = 500 \text{ ppm}$; $\text{NO}_2 = 50 \text{ ppm}$; $\text{O}_2 = 8\%$) at 120°C on $\text{BaO}/\text{Al}_2\text{O}_3$.

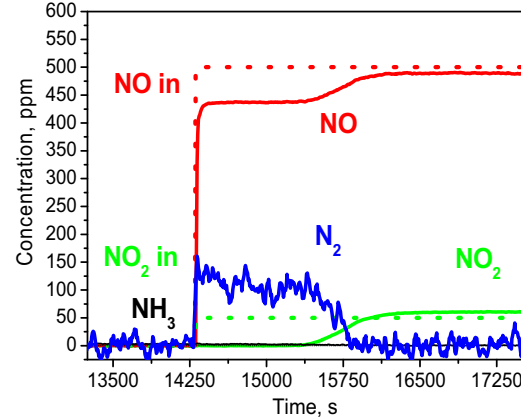


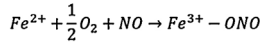
Fig. 8. Step feed of $\text{NO} + \text{NO}_2$ ($\text{NO} = 500 \text{ ppm}$; $\text{NO}_2 = 50 \text{ ppm}$; $T = 120^\circ\text{C}$;) following NH_3 adsorption at 120°C ($\text{NH}_3 = 500 \text{ ppm}$) on H-ZSM5.

be attributed to the NH_3 adsorbed on the zeolite acid sites, whereas the role of the NH_3 interaction with the Fe redox sites seems to be very limited at these conditions.

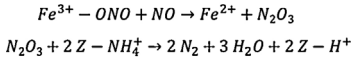
To further confirm these results, one additional, dual test was run on H-ZSM-5 only. The parent zeolite was first saturated with NH_3 at 120°C (not shown for brevity) and then, after NH_3 shutoff, a mixture of 500 ppm of NO and 50 ppm of NO_2 was fed to the reactor, still at the same temperature. **Fig. 8** shows the following isothermal transient: it is evident that, as soon as the NOx mixture was contacted with adsorbed NH_3 , already at 120°C NO_2 , i.e. the limiting reactant, was fully converted to N_2 . The corresponding NO conversion and N_2 release were in line with the stoichiometry of Fast SCR, Reaction (R3). Of course, after some time the preadsorbed NH_3 was depleted, and both NO and NO_2 eventually approached their steady-state levels. It is thus possible to conclude that $\text{NO} + \text{NO}_2$ in equilibrium with nitrites react with adsorbed NH_3 already at very low temperatures and with extremely fast rates.

Another important implication is that, at our investigated conditions, the formation of N_2 from $\text{NH}_3 + \text{NO} + \text{NO}_2$ may not necessarily require any oxidative activation of ammonia, given the extremely limited amount of Fe centers available on the H-ZSM-5 sample. This is consistent with data reported by Stakheev et al. [20] and by Ellmers et al. [21], showing the Fast SCR reaction to proceed on catalytic systems virtually free of redox sites. We are aware of the role of Fe impurities in determining the SCR activity of technical parent zeolites [21], such as the one used in this study. It is

Oxidation half cycle:



Reduction half cycle:



In addition:

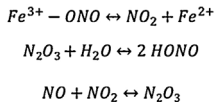


Fig. 9. Proposed redox chemistry for Standard SCR over Fe-zeolites.

worth emphasizing however that, in spite of a 40-times smaller load of iron in H-ZSM-5 than in the Fe-ZSM-5 catalyst, we obtained essentially the same high conversion activity observed on the Fe-promoted system already at low temperatures, as documented in Fig. 6. This seems therefore hardly compatible with a mechanism requiring the oxidative activation of NH₃ on Fe centers.

The very simple scheme in Fig. 9 provides a redox cycle, which is consistent with all the observations reported in this work.

Here, the reduced Fe sites are oxidized by oxygen and NO to form ferric nitrites, whose reductive decomposition leads to the release of NO₂, in equilibrium with N₂O₃ together with NO. In the presence of BaO, N₂O₃ will form Barium nitrites. In the presence of ammonia adsorbed on the zeolite acid sites, instead, N₂O₃ will form unstable ammonium nitrite, rapidly resulting in the evolution of N₂ and H₂O. Notably, this latter step does not involve any redox functionality, in agreement with our results in this section. It is also worth pointing out that NO₂ appears explicitly neither in the oxidation nor in the reduction half cycle in Fig. 9. NO oxidative activation leading to the reduction of Fe³⁺ in Fe-ZSM-5 has been observed by Boubnov et al. [22] by operando HERFD-XANES.

4. Conclusions

On investigating the effect of phase separation in Fe-ZSM-5 + BaO/Al₂O₃ combined systems exposed to NO/NO₂ + O₂ mixtures at 120 °C, we have collected a number of novel results which shed light on the NH₃-SCR catalytic chemistry over metal-promoted zeolites.

Our new data confirm the strong interaction between Fe-ZSM-5 and BaO/Al₂O₃, already documented in [12–14], but further prove that this proceeds via the gas phase. For NO + O₂ adsorption, in particular, the interaction is mediated by stable molecules, which act as nitrite precursors, resulting in nitrites storage on BaO, and are able to travel across the reactor even in the case of a fully segregated double bed configuration.

Concerning the nature of such mediating gaseous species, we have observed striking similarities between NO + O₂ adsorption on the Fe-ZSM-5 + BaO/Al₂O₃ mechanical mixture and NO₂ adsorption in excess NO on the sole BaO/Al₂O₃ phase. Therefore, it is tempting to conclude that the relevant mediating species is just NO₂. Indeed, while NO₂ alone has a formal N oxidation state of +4, we have shown that NO₂ in excess NO behaves instead as a nitrite precursor, i.e. with an N oxidation state of +3. We cannot rule out therefore that the gaseous intermediate generated by NO oxidation over Fe-ZSM-5 is actually another molecule with a formal N oxidation state of +3, like N₂O₃ or HONO. It is also possible that all such species, namely NO + NO₂, N₂O₃, HONO, are in equilibrium with each other, being eventually indistinguishable from a mechanistic and kinetic point of view. Regardless of the exact nature of the gaseous intermediate, our data point out very clearly that a crucial redox step in the Stan-

dard SCR mechanism at low temperatures involves the oxidation of the N atom in NO to a state of +3.

In addition, we have shown that nitrites generated by the oxidative activation of NO on Fe-ZSM-5 and stored on BaO react readily with NH₃ adsorbed on the zeolite acid sites via their decomposition to NO + NO₂. Most important, such a reactivity proceeds regardless of the concentration of redox metal sites on the zeolite: in fact, we have observed a quite comparable NH₃ reactivity with NO + NO₂ on Fe-ZSM-5 and on H-ZSM-5, in spite of the drastically reduced Fe content of the latter sample.

Altogether, the experiments herein presented mimic the two sequential steps of one possible low-temperature mechanistic pathway for the Standard SCR reaction over Fe-zeolites. In this bi-functional mechanism, the oxidative activation of NO on the Fe-sites provides the NO₂/N₂O₃/HONO gaseous reactive intermediates, which are then rapidly reduced to dinitrogen by the ammonia adsorbed on the catalyst acid sites. On the other hand, the oxidative activation of NH₃ was notably not necessary in our experiments in order to reduce NO to dinitrogen at 120 °C. While we cannot rule out other surface pathways, this gas-phase mediated route was found quite active and compelling at our experimental conditions.

Altogether, the present data suggest strong analogies with the Standard SCR mechanism postulated by Stakheev et al. [20] for their bifunctional Combicat systems, wherein one oxidative component is deemed responsible for the oxidation of NO to NO₂, while the other component, associated with acidic properties but not necessarily possessing redox properties, sustains the Fast SCR reactivity between NO, NO₂ and NH₃. In our experiments, however, both functionalities have been demonstrated for the same Fe-zeolite SCR catalyst. The novel evidence herein collected also emphasizes the often-overlooked potential relevance of gas-phase intermediates in the Standard SCR reaction over metal-promoted zeolites.

In all the present experiments, water was not added to the feed stream to the reactor, even though it is of course an important component of real engine exhausts, because we learnt from previous work [13] that water would significantly hamper the NO_x storage capability of BaO, and thus the efficiency of our chemical trapping techniques. A dedicated study of the H₂O effect will be reported however in the near future.

Acknowledgments

The authors acknowledge Mauro Fiorito and Alessandro Molina for the experimental work and for fervent discussions. ET is indebted to Wolfgang Grünert, Alexandr Stakheev and Alina Mytareva for stimulating discussions and critical suggestions.

References

- [1] S. Brandenberger, O. Kröcher, A. Tissler, R. Althoff, *Catal. Rev.—Sci. Eng.* 50 (2008) 492–531.
- [2] I. Ellmers, R.P. Vélez, U. Bentrup, A. Brückner, W. Grünert, *J. Catal.* 311 (2014) 199–211.
- [3] A. Grossale, I. Nova, E. Tronconi, D. Chatterjee, M. Weibel, *J. Catal.* 256 (2008) 312–322.
- [4] M.P. Ruggeri, I. Nova, E. Tronconi, *Top. Catal.* 56 (2013) 109–113.
- [5] A. Savara, M.-J. Li, W.M.H. Sachtler, E. Weitz, *Appl. Catal. B: Environ.* 81 (2008) 251–257.
- [6] A. Savara, W.M.H. Sachtler, E. Weitz, *Appl. Catal. B: Environ.* 90 (2009) 120–125.
- [7] Y.H. Yeom, J. Henao, M.J. Li, W.M.H. Sachtler, E. Weitz, *J. Catal.* 231 (2005) 181–193.
- [8] J.H. Kwak, J.H. Lee, S.D. Burton, A.S. Lipton, C.H.F. Peden, J. Szanyi, *Angew. Chem.—Int. Ed.* 52 (2013) 9985–9989.
- [9] C. Paolucci, A.A. Verma, S.A. Bates, V.F. Kispersky, J.T. Miller, R. Gounder, W.N. Delgass, F.H. Ribeiro, W.F. Schneider, *Angew. Chem.* (2014) 11828–11833.
- [10] T.V.W. Janssens, H. Falsig, L.F. Lundsgaard, P.N.R. Vennestøm, S.B. Rasmussen, P.G. Moses, F. Giordanino, E. Borfecchia, K.A. Lomachenko, C. Lamberti, S. Bordiga, A. Godiksen, S. Mossin, P. Beato, *ACS Catal.* 5 (2015) 2832–2845.
- [11] M. Schwidder, S. Heikens, A. De Toni, S. Geisler, M. Berndt, A. Brückner, W. Grünert, *J. Catal.* 259 (2008) 96–103.

- [12] M.P. Ruggeri, T. Selleri, M. Colombo, I. Nova, E. Tronconi, *J. Catal.* 311 (2014) 266–270.
- [13] M.P. Ruggeri, T. Selleri, M. Colombo, I. Nova, E. Tronconi, *J. Catal.* 328 (2015) 258–269.
- [14] T. Selleri, M.P. Ruggeri, I. Nova, E. Tronconi, *Top. Catal.* 59 (2016) 678–685.
- [15] M.P. Ruggeri, T. Selleri, I. Nova, E. Tronconi, J.A. Pihl, T.J. Toops, W.P. Partridge, *Top. Catal.* 59 (2016) 907–912.
- [16] M.P. Ruggeri, A. Grossale, I. Nova, E. Tronconi, H. Jirglova, Z. Sobalik, *Catal. Today* 184 (2012) 107–114.
- [17] M. Colombo, I. Nova, E. Tronconi, *Appl. Catal. B: Environ.* 111–112 (2012) 433–444.
- [18] M. Salazar, S. Hoffmann, O.P. Tkachenko, R. Becker, W. Grünert, *Appl. Catal. B: Environ.* 182 (2016) 213–219.
- [19] B.M. Weiss, K.B. Caldwell, E. Iglesia, *J. Phys. Chem. C* 115 (2011) 6561–6570.
- [20] A.Y. Stakheev, A.I. Mytareva, D.A. Bokarev, G.N. Baeva, D.S. Krivoruchenko, A.L. Kustov, M. Grill, J.R. Thøgersen, *Catal. Today* 258 (2015) 183–189.
- [21] I. Ellmers, R. Pérez Vélez, U. Bentrup, W. Schwieger, A. Brückner, W. Grünert, *Catal. Today* 258 (2015) 337–346.
- [22] A. Boubnov, H.W.P. Carvalho, D.E. Doronkin, T. Günter, E. Gallo, A.J. Atkins, C.R. Jacob, J.-D. Grunwaldt, *J. Am. Chem. Soc.* 136 (2014) 13006–13015.